

## Magnetic field sensor with voltage-tunable sensing properties

Witold Skowroński,<sup>1,a)</sup> Piotr Wiśniowski,<sup>1</sup> Tomasz Stobiecki,<sup>1</sup> Susana Cardoso,<sup>2</sup> Paulo P. Freitas,<sup>2</sup> and Sebastiaan van Dijken<sup>3</sup>

<sup>1</sup>Department of Electronics, AGH University of Science and Technology, Al. Mickiewicza 30, 30-059 Kraków, Poland

<sup>2</sup>INESC-MN and IN- Institute of Nanoscience and Nanotechnology, Lisbon 1000-029, Portugal

<sup>3</sup>NanoSpin, Department of Applied Physics, Aalto University School of Science, P.O. Box 15100, FI-00076 Aalto, Finland

(Received 28 August 2012; accepted 18 October 2012; published online 5 November 2012)

We report on a magnetic field sensor based on CoFeB/MgO/CoFeB magnetic tunnel junctions. By taking advantage of the perpendicular magnetic anisotropy of the MgO/CoFeB interface, the magnetization of the sensing layer is tilted out-of-plane which results in a linear magnetoresistance response to in-plane magnetic fields. The application of a bias voltage across the MgO tunnel barrier of the sensor affects the magnetic anisotropy and thereby its sensing properties. We propose a voltage-tunable magnetic field sensor design that allows for active control of the sensitivity and the operating field range by the strength and polarity of the applied bias voltage. © 2012 American Institute of Physics. [<http://dx.doi.org/10.1063/1.4765350>]

Magnetic tunnel junctions (MTJs) based on CoFeB electrodes separated by a MgO tunnel barrier are excellent candidates for magnetic memory cells,<sup>1</sup> magnetic field sensors, and microwave nano-electronics components,<sup>2,3</sup> due to a high tunneling magnetoresistance (TMR) ratio and easy control of their magnetization with either magnetic field or spin polarized current. Magnetic field sensors utilizing TMR or giant magnetoresistance (GMR) effects are often designed with an orthogonal alignment between the magnetizations of the sensing and reference layer (RL).<sup>4-7</sup> This cross configuration produces a linear and reversible magnetoresistance (MR) response by coherent rotation of the sensing layer magnetization in a perpendicular applied magnetic field. One viable way of realizing a magnetic cross geometry is the use of a sensing layer with out-of-plane magnetization.<sup>8</sup> The sensing properties of such MR sensors are usually fixed, and depending on the operating range and magnetic field sensitivity that are required for specific applications, different sensors are needed.

Recently, it was shown that the magnetic anisotropy of thin ferromagnetic layers can be modified by an applied electric field.<sup>9-11</sup> This feature was utilized in pseudo-spin valve structures to manipulate the MTJ resistance<sup>12</sup> and it was used to demonstrate electric-field control of prototype memory cells.<sup>13,14</sup> In addition, it was shown that resonance excitations of nanomagnets can be induced by electric fields alone.<sup>15</sup>

In this letter, we demonstrate that electric-field control of magnetic anisotropy in cross-magnetization-geometry MTJs enables the design of magnetic field sensors with voltage-tunable sensing properties. Our experiments are conducted on exchanged-biased CoFeB/MgO/CoFeB MTJs with a synthetic antiferromagnet (SAF). In the sensors, the CoFeB sensing layer is oriented out-of-plane due to the perpendicular magnetic anisotropy of the MgO/CoFeB interface.<sup>16,17</sup> In combination with the in-plane magnetic anisotropy of the CoFeB RL, this produces linear transfer curves. Moreover,

both the operating field range and the field sensitivity are controllable by the strength and polarity of the applied bias voltage. The ability to actively modify the sensing characteristics without the need of extra signal lines or other components opens the door to single adaptable field sensors that combine high sensitivity and large magnetic field ranges.

The thin-film magnetic field sensors of the following multilayer structure: Si/SiO<sub>2</sub>/Ta 5/Ru 18/Ta 3/Pt<sub>46</sub>Mn<sub>54</sub>18/Co<sub>82</sub>Fe<sub>18</sub> 2.2/Ru 0.9/(Co<sub>52</sub>Fe<sub>48</sub>)<sub>75</sub>B<sub>25</sub> 3/MgO 1.35/(Co<sub>52</sub>Fe<sub>48</sub>)<sub>75</sub>B<sub>25</sub> 1.55/Ru 5/Ta 5 (thickness in nm)<sup>18</sup> were deposited using a Nordiko 2000 magnetron sputtering system. Before microfabrication processing, the films were passivated with a 15 nm thick Ti<sub>10</sub>W<sub>90</sub>N<sub>2</sub> capping layer. The 1 × 1 in. wafers were patterned by direct writing laser lithography and ion beam milling, which resulted in 540 devices with a tunnel junction dimension ranging from 1.5 × 3 μm up to 4 × 36 μm. The patterned wafer was annealed in high vacuum at 340 °C, for 1 h in a magnetic field of 5 kOe. The MgO tunnel barrier thickness of 1.35 nm corresponded to a resistance area (RA) product of 90 kΩ μm<sup>2</sup>. Resistance vs. magnetic field loops were measured using a four-probe method. In this letter, positive voltage indicates electron transport from the bottom RL to the top sensing layer. The sensitivity of the sensor was measured directly using lock-in detection with synchronization to a weak (0.5 Oe) sinusoidal magnetic field on top of a bias field.

Based on the results in Fig. 1 of Ref. 18, we selected a CoFeB sensing layer thickness of 1.55 nm, so that the resistance hysteresis loop is completely closed and linear in a medium magnetic field range. This effect is caused by the perpendicular interface anisotropy of the thin CoFeB sensing layer on top of the MgO tunnel barrier.<sup>16</sup> Figure 1 presents normalized TMR vs. in-plane magnetic field curves for different bias voltages  $V_B$  across the MgO tunnel barrier. The junction area of this MTJ is 4.5 μm<sup>2</sup>. For this MTJ sensor, a linear and non-hysteretic resistance change is observed for all investigated  $V_B$ . The TMR ratio measured at low  $V_B$  reaches 47% and drops to 24% for  $V_B = 1$  V. The polarity

<sup>a)</sup>Electronic address: skowron@agh.edu.pl.

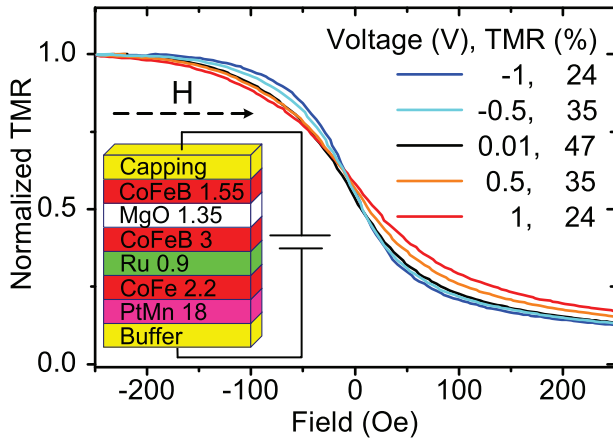


FIG. 1. Normalized TMR vs. in-plane magnetic field for different bias voltages. The strength and polarity of the bias voltage alter the perpendicular magnetic anisotropy of the CoFeB sensing layer, which is reflected by a change in the shape of the TMR curves. Inset: the MTJ structure with a bias voltage.

and magnitude of the applied bias voltage affect the magnetic anisotropy of the thin CoFeB sensing layer.<sup>10,11,13</sup> Positive bias voltages increase the out-of-plane magnetic anisotropy. As a consequence, the magnetization of the sensing layer rotates less when an in-plane magnetic field is applied and this increases the field range of the linear TMR response. Negative voltages reduce the out-of-plane anisotropy of the CoFeB layer and this results in a more sensitive sensor response. We note that the current density in the smallest MTJ sample only amounts to  $9 \times 10^2$  A/cm<sup>2</sup> under maximum bias conditions. This is three orders of magnitude smaller than the current density that is typically required for spin-transfer-torque (STT) induced resistance changes.<sup>19</sup> STT effects can, therefore, be excluded in this study.

Figure 2 shows normalized TMR vs. in-plane magnetic field loops measured with  $V_B = \pm 1$  V together with linear fits of the sensor response in small applied magnetic field. The linear operating range, defined as the field range in which the sensor response is linear within 2% error, changes from  $\pm 36$  Oe for  $V_B = -1$  V, up to  $\pm 69$  Oe for  $V_B = 1$  V. The maximum field sensitivity defined as the change of the TMR

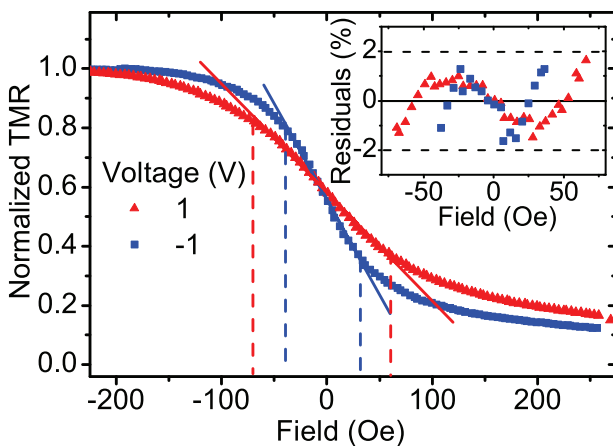


FIG. 2. Normalized TMR vs. in-plane magnetic field curves for  $V_B = \pm 1$  V. The solid lines represent linear fits and the dashed lines indicate the linear operating range. The field sensitivity is 0.082%/Oe and 0.149%/Oe for  $V_B = 1$  V and  $V_B = -1$  V, respectively. Inset: linear fit residuals of the sensor vs. magnetic field curves within the operating range.

ratio divided by the linear operating range drops from 0.149%/Oe for  $V_B = -1$  V, to 0.082%/Oe for  $V_B = 1$  V. Similar results were obtained by direct sensitivity measurements as illustrated in Fig. 3. In these experiments, the MTJ was placed in a sinusoidal magnetic field of  $H_{AC} = 0.5$  Oe. This produced an AC output signal, whose amplitude increased from 47  $\mu$ V/V/Oe for  $V_B = 1$  V, up to 89  $\mu$ V/V/Oe for  $V_B = -1$  V. The MTJs with voltage-tunable TMR properties can be used as smart sensors that operate in different field ranges. The breakdown voltage of the MTJs exceeds 2 V and, therefore, the changes in the operating field range and sensitivity are obtained well below breakdown events. The other sensors on the wafer with different junction areas exhibit the same behavior, which is consistent with theoretical predictions that electric-field-induced changes are independent of junction size.

To estimate the change of perpendicular magnetic anisotropy in an applied electric field, we performed an analysis that is similar to the one presented in Ref. 12. In this procedure, the ratio of the in-plane magnetization component  $M_{in}$  to the total magnetization  $M$  was estimated from the dependence of the resistance  $R$  on the angle  $\theta$  between the magnetization of the sensing layer and RL

$$R = R_p + \frac{R_{ap} - R_p}{2} \left( 1 - \frac{M_{in}}{M} \right), \quad (1)$$

where  $R_p$  and  $R_{ap}$  are the resistances for parallel and antiparallel magnetization states, respectively, and  $M_{in}/M = \cos \theta$ . The perpendicular anisotropy energy was calculated by integrating  $M_{in}/M$  over the measured field range from 0 to 2500 Oe, which corresponds to the in-plane saturation field of the CoFeB sensing layer. An example of the integration area for  $V_B = -0.5$  V is presented in the inset of Fig. 4. In our calculation, we used  $\mu_0 M_s = 0.93$  T for the 1.55 nm thick  $(\text{Co}_{52}\text{Fe}_{48})_{75}\text{B}_{25}$  sensing layer.

As shown in Fig. 4, the perpendicular magnetic anisotropy energy of a  $4.5 \mu\text{m}^2$  sensor without  $V_B$  applied is  $E_{\text{perp}t_{FL}} = 101 \mu\text{J}/\text{m}^2$ . This energy changes approximately linearly with applied electric field. The linear field dependence corresponds to 19 fJ/Vm, which is in good agreement

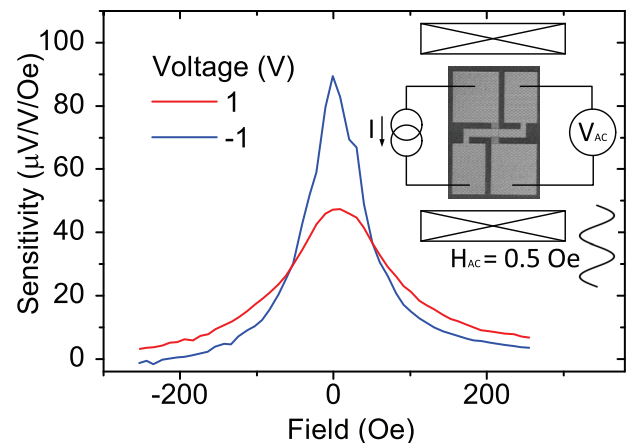


FIG. 3. Sensitivity of the magnetic field sensor measured for  $V_B = \pm 1$  V, using a four-probe lock-in detection scheme (shown in the inset). The maximum sensitivity, measured for  $H = 0$  Oe, increases by a factor of two when the polarity of the 1 V bias voltage is reversed.

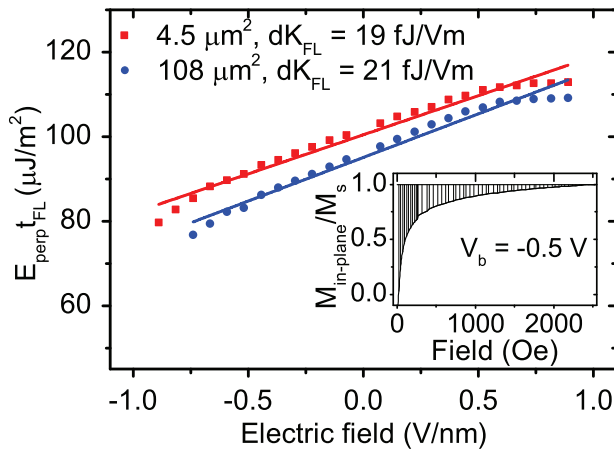


FIG. 4. Perpendicular magnetic anisotropy energy of the CoFeB sensing layer as a function of applied electric field. The data were extracted by integrating  $M_{in}/M_s$  vs. magnetic field curves for MTJs with an area of  $4.5 \mu\text{m}^2$  and  $108 \mu\text{m}^2$  (inset).

with sputter-deposited and annealed CoFeB layers<sup>11</sup> and crystalline CoFe.<sup>12</sup> For sensors with larger junction areas, similar values were obtained.

In summary, we have demonstrated a magnetic field sensor concept with voltage-tunable operating field range and sensitivity. The sensor consists of a MgO-based magnetic tunnel junction with a perpendicular CoFeB sensing layer. The anisotropy strength depends linearly on the bias voltage across the MgO tunnel barrier. As a result, a wide range of sensing properties can be realized in one integrated device. In our proof of concept experiments, the measurement range and field sensitivity are enhanced by a factor of two when the polarity of the bias voltage is switched. These unique features are relevant for magnetic field sensor designs with multiple sensing functions.

T.S. and W.S. acknowledge the Foundation for Polish Science MPD Programme co-financed by the EU European Regional Development Fund. This work was supported by the Polish National Science Center grants (NN505489040, 11.11.120.614 and E-CONTROL-2012/04/M/ST7/00799),

FCT through the PIDDAC Program and Portuguese National Project PTDC/CTM-NAN/110793/2009. S.v.D. acknowledges financial support from the Academy of Finland (SA 127731).

- <sup>1</sup>R. Takemura, T. Kawahara, K. Miura, H. Yamamoto, J. Hayakawa, N. Matsuzaki, K. Ono, M. Yamanouchi, K. Ito, H. Takahashi, S. Ikeda, H. Hasegawa, H. Matsuoka, and H. Ohno, *IEEE J. Solid-State Circuits* **45**(4), 869–879 (2010).
- <sup>2</sup>A. Dussaux, B. Georges, J. Grollier, V. Cros, A. Khvalkovskiy, A. Fukushima, M. Konoto, H. Kubota, K. Yakushiji, S. Yuasa, K. Zvezdin, K. Ando, and A. Fert, *Nat. Commun.* **1**(1), 8 (2010).
- <sup>3</sup>W. Skowroński, T. Stobiecki, J. Wrona, G. Reiss, and S. van Dijken, *Appl. Phys. Express* **5**(6), 063005 (2012).
- <sup>4</sup>M. Tondra, J. M. Daughton, D. Wang, R. S. Beech, A. Fink, and J. A. Taylor, *J. Appl. Phys.* **83**(11), 6688–6690 (1998).
- <sup>5</sup>X. Liu, C. Ren, and G. Xiao, *J. Appl. Phys.* **92**(8), 4722–4725 (2002).
- <sup>6</sup>Y. Lu, R. A. Altman, A. Marley, S. A. Rishton, P. L. Trouilloud, G. Xiao, W. J. Gallagher, and S. S. P. Parkin, *Appl. Phys. Lett.* **70**(19), 2610–2612 (1997).
- <sup>7</sup>D. Lacour, H. Jaffres, F. N. V. Dau, F. Petroff, A. Vaures, and J. Humbert, *J. Appl. Phys.* **91**(7), 4655–4658 (2002).
- <sup>8</sup>S. van Dijken and J. M. D. Coey, *Appl. Phys. Lett.* **87**(2), 022504 (2005).
- <sup>9</sup>M. Weisheit, S. Fahler, A. Marty, Y. Souche, C. Poinsignon, and D. Givord, *Science* **315**(5810), 349–351 (2007).
- <sup>10</sup>T. Maruyama, Y. Shiota, T. Nozaki, K. Ohta, N. Toda, M. Mizuguchi, A. A. Tulapurkar, T. Shinjo, M. Shiraishi, S. Mizukami, Y. Ando, and Y. Suzuki, *Nat. Nanotechnol.* **4**(3), 158–161 (2009).
- <sup>11</sup>M. Endo, S. Kanai, S. Ikeda, F. Matsukura, and H. Ohno, *Appl. Phys. Lett.* **96**(21), 212503 (2010).
- <sup>12</sup>Y. Shiota, S. Murakami, F. Bonell, T. Nozaki, T. Shinjo, and Y. Suzuki, *Appl. Phys. Express* **4**(4), 043005 (2011).
- <sup>13</sup>Y. Shiota, T. Nozaki, F. Bonell, S. Murakami, T. Shinjo, and Y. Suzuki, *Nature Mater.* **11**(1), 39–43 (2011).
- <sup>14</sup>W.-G. Wang, M. Li, S. Hageman, and C. L. Chien, *Nature Mater.* **11**(1), 64–68 (2011).
- <sup>15</sup>T. Nozaki, Y. Shiota, S. Miwa, S. Murakami, F. Bonell, S. Ishibashi, H. Kubota, K. Yakushiji, T. Saruya, A. Fukushima, S. Yuasa, T. Shinjo, and Y. Suzuki, *Nat. Phys.* **8**(6), 492–497 (2012).
- <sup>16</sup>S. Ikeda, K. Miura, H. Yamamoto, K. Mizunuma, H. D. Gan, M. Endo, S. Kanai, J. Hayakawa, F. Matsukura, and H. Ohno, *Nature Mater.* **9**(9), 721–724 (2010).
- <sup>17</sup>P. Wiśniowski, J. Wrona, T. Stobiecki, S. Cardoso, and P. P. Freitas, *IEEE Trans. Magn.* **48**(11), 3840 (2012).
- <sup>18</sup>P. Wiśniowski, J. M. Almeida, S. Cardoso, N. P. Barradas, and P. P. Freitas, *J. Appl. Phys.* **103**(7), 07A910 (2008).
- <sup>19</sup>W. Skowroński, T. Stobiecki, J. Wrona, K. Rott, A. Thomas, G. Reiss, and S. van Dijken, *J. Appl. Phys.* **107**(9), 093917 (2010).